Journal of the Serbian Chemical Society
JSCS-info@shd.org.rs • www.shd.org.rs/JSCS
J. Serb. Chem. Soc. *85* (8) 1033–1046 (2020) UDC 542.9+547.571'551:577.164.1+546.562:519.677:539.196
JSCS–5357
Original scientific paper

(*E*)-4-(((2-Amino-5-chlorophenyl)imino)methyl)-5-(hydroxymethyl)-2-methylpyridin-3-ol and its Cu(II) complex: Synthesis, DFT calculations and AIM analysis

MORTEZA YAVARI, S. ALI BEYRAMABADI*, ALI MORSALI and MOHAMMAD REZA BOZORGMEHR

Department of Chemistry, Mashhad Branch, Islamic Azad University, Mashhad, Iran

(Received 10 October 2019, revised 6 April, accepted 26 April 2020)

Abstract: Herein, (*E*)-4-{[(2-amino-5-chlorophenyl)imino]methyl}-5-(hydroxymethyl)-2-methylpyridin-3-ol [**HL**] Schiff base and its [Cu(L)Cl] complex were newly synthesized and characterized by several spectroscopic methods. In addition, density functional theory (DFT) methods were used for investigation of the tautomerization of the **HL** Schiff base, structural parameters of **HL** and [Cu(L)Cl] species, assignment of the IR vibrational bands and the NMR chemical shifts as well as natural bond orbital (NBO) analyses. The most stable tautomer of the **HL** Schiff base is the enol form of the meta isomer. The optimized geometry of the free **HL** Schiff base is not planar. The $\mathbf{L}^-$ acts as a N_2O tridentate ligand, which is bonded to Cu^{2+} *via* the deprotonated phenolic oxygen, and the amine and azomethine nitrogens. The [Cu(**L**)Cl] has a square planar geometry in which the chloro ligand occupies the fourth coordination position. The DFT-computed values are in good consistency with the corresponding experimental values, confirming the suitability of the optimized geometries for **HL** and [Cu(**L**)Cl] species. According to the high-energy gaps, these compounds are stable. The atoms in molecule (AIM) analysis was used to evaluate strength of the bonding interactions and electron densities in structure of the compounds.

Keywords: Schiff base; pyridoxal; DFT; copper(II); AIM; tautomerization.

INTRODUCTION

Easy preparation and variety in structure make Schiff bases the most versatile studied ligands in coordination chemistry.[1–4] On the other hand, due to many useful applications, such as analytical agent[5] and industrial use as catalysts,[6,7] Schiff bases and their metal complexes are of great importance. Especially, this large family of chemical compounds has been shown to have significant bio-

* Corresponding author. E-mails: beiramabadi6285@mshdiau.ac.ir; beiramabadi@yahoo.com
https://doi.org/10.2298/JSC191010022Y

logical activities, such as antibacterial,[3,4,8] antifungal,[8] anticancer and antioxidant[2,9] activities.

Cu(II) Schiff base complexes exhibit important biological activities, such as antifungal and antimicrobial properties,[3,8] interaction with DNA[1,10,11] as well as considerable anti-tumor activities against a broad spectrum of cancers.[10,12] In addition, these complexes show considerable catalytic properties.[13,14]

Nowadays, DFT methods are extensively used to explore many areas of chemical compounds and chemical reactions, such as the characterization of the molecular structures, spectroscopic assignments, drug design, kinetics and mechanism of reactions, *etc*.[1,12,15]

In this work, pyridoxal, which is a close analogue of the vitamin B_6,[6] was the used aldehyde.[1] Systems containing pyridoxal or pyridoxamine mimic enzymatic reactions. Since vitamin B6–metal complexes have been extensively investigated as models of enzymatic behavior,[17,18] metal complexes of pyridoxal are also of interest in view of their significant biological activities.[19] Previously, several studies were reported on the synthesis, characterization and properties of Schiff bases derived from the condensation reaction between pyridoxal and several aliphatic and aromatic diamines.[15,20–24] Among them, 4-((*E*)-(2-amino-5-nitrophenylimino)methyl)-5-(hydroxymethyl)-2-methylpyridin-3-ol Schiff base was the only tridentate ligand, which is attributed to the $–NO_2$ electron withdrawing agent in the structure of 4-nitro-*o*-phenylenediamine.[22] In this work, the (*E*)-4-(((2-amino-5-chlorophenyl)imino)methyl)-5-(hydroxymethyl)-2-methylpyridin-3-ol [=**HL**] tridentate Schiff base of the pyridoxal as well as its copper(II) complex were newly synthesized. In addition to several experimental characterizations, the synthesized compounds were identified theoretically by employing valuable DFT methods. Another aim of this work was the identification of the bonding interactions and electron density of the rings using AIM analysis.

EXPERIMENTAL

Material and methods

All of the used chemicals were obtained from the Merck Company. They were used as received. The melting points of the samples were determined using an electrothermal 9100 melting point apparatus. A Bruker Tensor 27 spectrophotometer was employed to record the IR spectra as KBr disks. The CHN elemental analysis was realized on a Heraeus elemental analyzer CHN-O-Rapid. In addition, the percentage of Cu^{2+} metal ion was measured using a Hitachi 2-2000 atomic absorption spectrophotometer. The ^{1}H- and ^{13}C-NMR spectra were recorded on a Varian-400 MHz (USA) spectrometer in DMSO solvent using tetramethylsilane (TMS) as the reference. The mass spectra were recorded on a Shimadzu-GC-Mass-Qp 1100 Ex, using the atmospheric pressure chemical ionization (ACPI) method.

*Synthesis of the **HL** Schiff base*

A solution of 10 mmol NEt_3 in 5 mL methanol was added to a solution of pyridoxal hydrochloride (10 mmol, 2.036 g) in 8 mL methanol. The obtained solution was stirred for 10 min. Then, a solution of 4-chloro-*o*-phenylenediamine (10 mmol, 1.426 g) in 10 mL methanol

was slowly added to the pyridoxal solution. The obtained mixture was stirred for 4 h at room temperature. Then, the yellow solid of the **HL** Schiff base was filtered off, washed with cold methanol and dried in air (yield: 88 % and Dec. Temp.: 224 °C).

*Synthesis of the [Cu(**L**)Cl] complex*

The **HL** Schiff base (2 mmol, 0.583 g) dissolved in 20 mL methanol and then a solution of 2 mmol (0.341 g) $CuCl_2 \cdot 2H_2O$ in 10 mL methanol was added dropwise. Five drops of triethylamine were used to catalyze separation of the phenolic proton. The mixture was refluxed for 3 h. The obtained brown precipitate of [Cu(**L**)Cl] was filtered, washed with methanol and recrystallized from acetonitrile (Yield: 71 % and Dec. Temp.: 211 °C).

Computational details

In this work, all the calculations were performed by employing the Gaussian 03 program and valuable DFT methods.[25] The M062X functional[26] and 6-311+G(d,p) basis set were used except for the Cu metal atom, where the LANL2DZ basis set[27] was employed together with its effective core potential functions.

Firstly, the geometries of the investigated species were fully optimized. The gas phase optimized geometries showed no imaginary frequency of the Hessian, except for the transition states (TSs), which had one imaginary frequency. This approves the suitability of the optimized geometries for the investigated species. The tautomerization reaction of the **HL** Schiff base was explored in both the gas phase and methanol solution. The polarizable-continuum model (PCM)[28] was used to consider the solvent effects. The zero-point energy and thermal corrections were considered in the evaluation of the electronic energies and the Gibbs free energies.

The NMR and IR calculations as well as the Natural Bond Orbital (NBO) analysis were performed on the optimized geometries at the same computational level. The ^{1}H- and ^{13}C-NMR chemical shifts of the **HL** Schiff base were predicted in DMSO solution with respect to the TMS by employing the gauge-independent atomic orbital (GIAO) method.[29] Usually, the DFT-computed IR frequencies are higher than the experimental one. Since, the DFT-computed vibrational frequencies were improved by a scale factor of 0.9614.[30] The Fukui functions are an important concept in the DFT, which have been extensively used in prediction of reactive site of compounds. Herein, the isosurface Fukui maps were computed by employing Multiwfn-3.6 software.[31]

In addition, the quantum theory of atoms in molecules (QTAIMs) was employed to explore character of important bonds and rings. The AIMALL package[32] was used for the QTAIM calculations. These calculations were based on the topological analysis of the electron density, $\rho(r)$.[33] Several quantities are correlated to the $\rho(r)$, such as the kinetic energy density (G_b), the potential energy density (V_b), the total energy density (H_b) and the Laplacian of the electron density $\nabla^2\rho$ at a bond critical point (BCP). These quantities are applicable for investigation on the nature of bonds. The strength of a bond is determined by its molecular electronic charge density ($\rho(r)$). The hydrogen bond energies can be computed by $E_{HB} = = 1/2V_b$.[34] Additionally, the signs of $\nabla^2\rho$ and H_b at a BCP give additional information about the nature of the interactions. If ($\nabla^2\rho < 0$, $H_b < 0$), ($\nabla^2\rho > 0$, $H_b < 0$) and ($\nabla^2\rho > 0$, $H_b > 0$), the investigated interaction will be strong, medium and weak, respectively. Furthermore, the $-G_b/V_b$ value is a criterion to characterize a bond, where $-G_b/V_b > 1$, $0.5 < -G_b/V_b > 1$ and $-G_b/V_b < 0.5$ values are attributed to non-covalent, partially covalent and covalent interactions, respectively.[35]

RESULTS AND DISCUSSION

Analysis of the investigated species

The CHN elemental analysis results of the investigated species are gathered in Table S-I of the Supplementary material to this paper. Good consistency between the calculated and experimental values confirms the validity of the proposed formulas for the **HL** Schiff base and its [Cu(**L**)Cl] complex. Furthermore, the obtained values for percentage of Cu^{2+} in the structure of the complex is in good consistency with the proposed formula for the [Cu(**L**)Cl] complex (Table S-I). In addition to the elemental analysis, the molecular ion peaks in the mass spectra of the **HL** Schiff base and [Cu(**L**)Cl] appear at 290 and 385 *m*/*z*, respectively. This is further evidence supporting the proposed formulas for the investigated species.

Geometry optimization

*Geometry and tautomerism of **HL**.* The elemental analysis indicates that only one of the amine groups of the 4-chloro-orthophenylenediamine reactant contributes in the condensation reaction with one pyridoxal molecule to produce the **HL** Schiff base. Since, the **HL** Schiff base may exist as two isomers, *para* and *meta*, the structures of these isomers are shown in Fig. 1. As seen, for formation of the *para* isomer, the *para* $-NH_2$ group of the used diamine reacts with the –CHO group of the pyridoxal to produce the C4=N2 azomethine group.

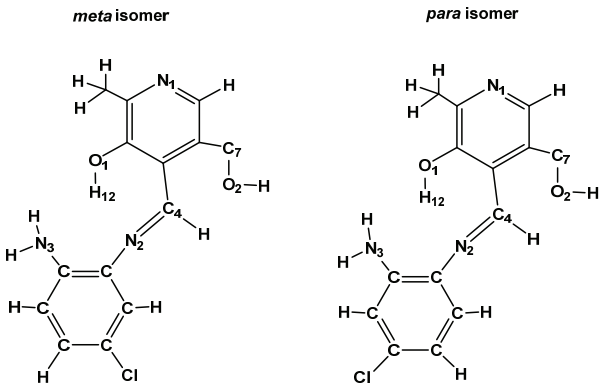

Fig. 1. Structures of the *para* and *meta* isomers of the **HL** Schiff base.

However, in the *meta* isomer, the *meta* $-NH_2$ group with respect to the chloro substituent reacts with the –CHO group. The **HL** Schiff base involves a phenolic proton (H12) that can transfer between the phenolic oxygen (O1) and nitrogen atom of the –C=N azomethine group (N2). This intramolecular-proton transfer (IPT) results in tautomerization of the **HL** Schiff base. Since, each of the *para* and *meta* isomers of the **HL** Schiff base could exist as two different tau-

tomers, enol and keto, the fully optimized geometries of both tautomers of the *para* and *meta* isomers are shown in Figs. 2 and 3, respectively.

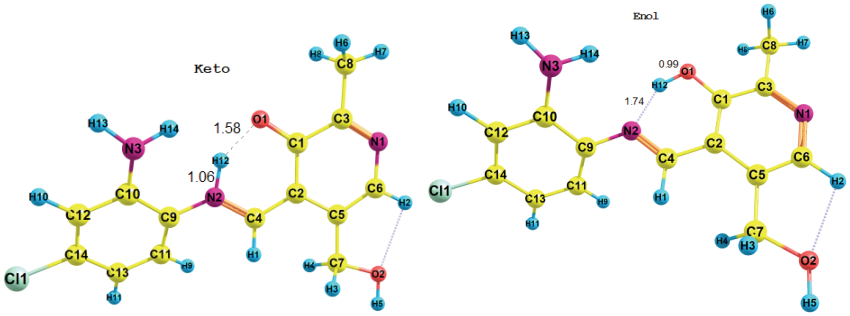

Fig. 2. Optimized geometries of the enol and keto tautomers of the *para* isomer.

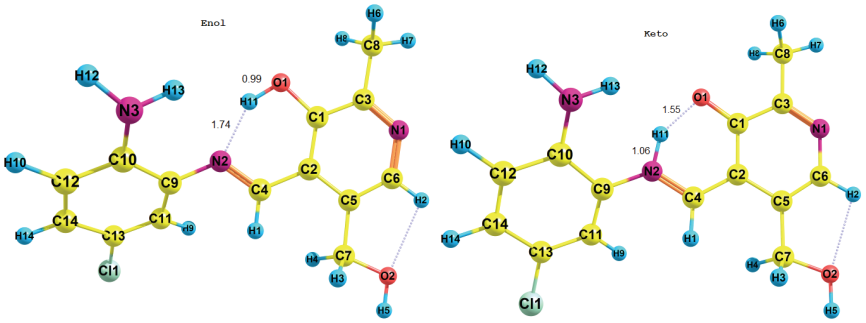

Fig. 3. Optimized geometries of the enol and keto tautomers of the *meta* isomer.

The electronic and Gibbs energy changes of the investigated species were evaluated with consideration of thermal corrections. The sum of the electronic and the zero-point energies (*E*+*ZPE*) indicate that the tautomers of the *meta* isomer are more stable than the corresponding tautomers of the *para* isomer. Since, methanol solution of the **HL** Schiff base involves only the *meta* isomer, the calculated values for the Gibbs energy change (ΔG) also approve this matter (Table S-II of the Supplementary material). The chloro substitution deactivates the *ortho* and *para* positions of the benzene ring for nucleophilic attack of the carbonyl group. As seen in Table S-II, the energies of the investigated species are reduced by considering the solvent effects in the PCM model.

The enol tautomer of the *meta* isomer is more stable than its keto tautomer. The transition state of the enol–keto tautomerization of the *meta* isomer was named as TSEnol–Keto. In its optimized geometry, breaking of the O1–H12 bond and formation of the N2–H12 bond is clear (Fig. S-1 of the Supplementary material). The activation energy (E_a) for the enol–keto tautomerization of the *meta* isomer is about 163 kJ mol^{-1}. Due to the large barrier energy, the enol tau-

tomer can not convert to the keto form. This is in good consistent with reported results for a similar Schiff base derived from the condensation reaction of 4-nitro-*o*-phenylenediamine and pyridoxal.[22]

*Geometry of the [Cu(**L**)Cl] complex.* As seen in Table S-I, the CHN elemental analysis as well as the molecular ion peaks of the mass spectra confirm that the synthesized Cu(II) complex has the [Cu(**L**)Cl] formula. Firstly, the **HL** Schiff base loses the H12 phenolic proton to produce the anionic $\mathbf{L}^-$ species. Then, $\mathbf{L}^-$ acts as a N_2O tridentate ligand. The optimized geometry of $\mathbf{L}^-$ is shown in Fig. S-2 of the Supplementary material. Due to deprotonation, the C1–O1 bond of the $\mathbf{L}^-$ species (126.1 pm) is shorter than the **HL** Schiff base (134.1 pm). The f^- Fukui function of the $\mathbf{L}^-$ ligand was computed to predict its electrophilic sites. As seen in Fig. S-2, the Fukui map is mainly localized on the phenolate oxygen (O1) and somewhat on the azomethine nitrogen (N2) atoms, which are the more suitable sites for coordination to metal ions.

The optimized geometry of the [Cu(**L**)Cl] complex is shown in Fig. 4, with labeling of the atoms. The important structural parameters of the enol tautomer of the *meta* isomer and the [Cu(**L**)Cl] complex are collected in Table I. The free **HL** Schiff base does not have a planar geometry; but the pyridine and benzene rings make a dihedral angle of about 40° with each other. The $\mathbf{L}^-$ ligand exhibits a more planar structure in the optimized geometries of the [Cu(**L**)Cl] complex, where the aromatic rings have a dihedral angle of only about 10° with each other.

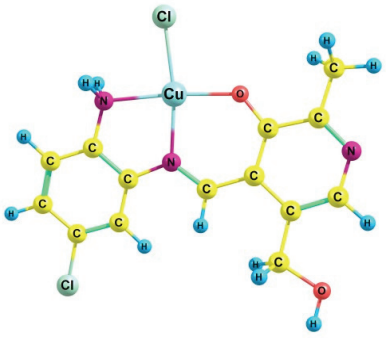

Fig. 4. The M062X optimized geometry of the [Cu(**L**)Cl] complex.

For example, see the calculated values for the C4–N2–C9–C11 and C4–N2–C9–C10 dihedral angles in Table I. The $\mathbf{L}^-$ ligand is coordinated to Cu^{2+} *via* the deprotonated-phenolic oxygen (O1), the azomethine nitrogen (N2) and the amine nitrogen (N3). The benzene ring rotates around the C9–N2 single bond to provide suitable conditions for chelation of the $\mathbf{L}^-$ ligand to Cu^{2+}. The fourth coordination position of the square planar complex is occupied by a chloro ligand.

Calculated dihedral angles in Table I confirm that four coordinating atoms are roughly in the same plane with Cu^{2+}. In the free **HL** Schiff base, the C9–N2

(140.9 pm) and C4–N2 (128.1 pm) bond lengths are in the range of a C–N single bond and a C=N double bond, respectively. In comparison with the free **HL** ligand, the coordination of the N2 and N3 atoms to Cu^{2+} elongates the C4–N2 and C10–N3 bonds, respectively. However, the O1 phenolic oxygen is deprotonated before coordination, which decreases the C1–O1 bond length in the complex compared to that in the free **HL** Schiff base. In the free **HL** Schiff base and [Cu(**L**)Cl], all substituents are essentially in the same plane with the corresponding aromatic ring. The C4=N2 azomethine group is in the same plane with the pyridine ring. The calculated structural parameters for two investigated species are in good consistency with the reported values for similar compounds.[1,4,8,12,15,20–24,36–39]

TABLE I. Selected structural parameters of the **HL** Schiff base and the [Cu(**L**)Cl] complex

Species	**HL**	complex	Species	**HL**	complex	Species	**HL**	complex
	Bond length, pm			Angle, °			Dihedral angle, °	
O1–H12	98.2	–	N2–H12–O1	145.7	–	N2–H12–O1–C1	5.6	–
H12–N2	177.3	–	H12–O1–C1	107.7	–	H12–O1–C1–C2	–1.1	–
N2–O1	264.3	283.5	O1–C1–C3	117.3	116.8	O1–C1–C2–C4	0.4	2.2
C4–N2	128.1	131.5	C1–C3–C8	119.2	118.5	C1–C2–C4–N2	–3.4	–0.3
C4–C2	146.0	142.1	C1–C3–N1	121.4	122.0	O1–C1–C3–C8	–0.1	–0.8
C2–C1	140.1	143.6	C6–C5–C7	120.9	120.4	O1–C1–C3–N1	179.8	178.8
C1–O1	134.1	128.9	C5–C7–O2	109.2	109.8	C1–C3–N1–C6	0.2	0.1
C1–C3	141.2	145.6	O1–C1–C2	123.3	125.7	C2–C5–C7–O2	–179.4	–179.5
C3–N1	132.0	131.3	C1–C2–C4	120.9	122.1	C5–C2–C4–N2	177.0	–179.6
C3–C8	150.0	150.2	C2–C4–N2	122.5	126.9	C2–C4–N2–C9	176.4	177.5
C5–C7	151.0	151.5	C4–N2–C9	119.9	122.0	C4–N2–C9–C10	140.4	171.3
C7–O2	141.1	142.1	N2–C9–C10	117.5	116.3	N2–C9–C10–N3	–5.6	0.4
C9–N2	140.9	141.1	C9–C10–N3	120.2	116.5	C9–C10–N3–H14	18.9	–113.8
C9–C10	140.9	141.0	C9–C10–C12	118.3	120.9	N2–C9–C10–C12	178.2	179.8
C10–N3	138.4	144.7	C14–C13–Cl1	120.6	120.8	C9–C10–C12–C14	–0.6	–0.4
C13–Cl1	174.5	175.4	N2–C9–C11	122.1	125.3	C12–C14–C13–Cl1	–179.0	179.7
N2–N3	275.7	268.2	O1–Cu–N2	–	92.3	C4–N2–C9–C11	–42.5	–10.1
Cu–O1	–	192.2	O1–Cu–N3	–	174.0	O1–N2–N3–Cu	–	1.5
Cu–N2	–	201.0	N2–Cu–N3	–	82.2	O1–N2–N3–Cl2	–	2.5
Cu–N3	–	207.1	N3–Cu–Cl2	–	88.2	C2–C1–O1–Cu	–	2.6
Cu–Cl2	–	227.5	N2–Cu–Cl2	–	170.3	Cl2–Cu–N2–C9	–	–1.2

Yang and co-workers[40] proposed a geometry index (τ_4) for four-coordinated complexes. The τ_4 index is obtained from the equation $\tau_4 = (360 - (\alpha+\beta))/141$, where α and β are the two largest θ angles around the central metal ion. The value of τ_4 varies from zero for the perfect square planar geometry to 1.00 for the perfect tetrahedral one, with intermediate structures (*e.g.* trigonal pyramidal or seesaw) in between. To explore the geometry of [Cu**L**Cl], its τ_4 index was calculated. In [Cu**L**Cl], the N3–Cu–Cl and N1–Cu–O1 angles are 170.3 and 174.0°, respectively. These angles are considered as the alpha and beta angles. The τ_4

index of the complex is 0.11, which confirms that geometry of [Cu**L**Cl] is very close to square planar.

*NMR spectrum of the H**L***

The ^{1}H- and ^{13}C-NMR spectra of the **HL** Schiff base are shown in Fig. S-3 of the Supplementary material. For comparison, the NMR chemical shifts (δ) were calculated for possible tautomers of the *para* and *meta* isomers. The experimental and DFT-computed ^{1}H- and ^{13}C-NMR chemical shifts (δ) of the **HL** Schiff base are gathered in Table II, where the atom positions are numbered as in Figs. 2 and 3. As seen, the experimental chemical shifts are in good consistency with the DFT-calculated chemical shifts for the enol tautomer of the *meta* isomer. In addition to the calculated E+ZPE and ΔG values, the calculated NMR-chemical shifts approve that a methanol solution of the **HL** Schiff base involves only the enol tautomer of the *meta* isomer.

TABLE II. The experimental and DFT-computed ^{1}H- and ^{13}C-NMR chemical shifts (δ / ppm) of the HL Schiff base in DMSO solution

^{1}H-NMR						^{13}C-NMR					
Atom position	Exp.	Theoretical				Atom position	Exp.	Theoretical			
		meta		*para*				*meta*		*para*	
		Enol	Keto	Enol	Keto			Enol	Keto	Enol	Keto
H12	13.48	13.30	18.47	11.52	18.61	C4	160.40	164.74	156.97	165.83	154.35
H1	9.07	9.36	8.97	9.43	9.03	C1	159.75	158.65	178.48	156.19	178.55
H2	8.01	8.07	8.19	9.01	8.20	C3	153.15	156.64	166.87	155.79	166.76
H9	7.10	7.70	7.86	7.55	7.90	C10	150.92	148.19	142.20	144.66	142.34
H10	6.87	7.16	7.62	7.49	7.50	C6	150.28	147.11	135.45	143.82	135.71
H11	6.69	7.03	7.44	7.22	7.28	C9	142.61	144.89	136.18	144.05	134.29
H4	5.54	5.35	5.02	5.26	5.04	C5	138.69	137.28	133.11	135.59	133.29
H3		5.21	5.02	5.12	5.04	C14	133.94	136.85	136.28	146.90	147.17
H14	4.79	4.68	4.57	4.71	4.74	C13	124.10	124.20	122.44	118.46	112.65
H13		3.86	4.24	3.81	4.28	C11	120.95	121.93	121.50	123.20	123.62
H6	2.46	2.71	2.65	2.65	2.65	C2	120.49	120.18	111.66	118.44	110.83
H8		2.71	2.65	2.65	2.65	C12	113.79	117.59	117.40	114.15	115.08
H7		2.44	2.12	2.37	2.11	C7	58.87	57.99	55.80	56.94	55.90
H5	5.44	1.53	1.30	1.44	1.31	C8	19.23	17.42	18.40	17.51	18.29

The DFT-chemical shift for the H5 proton of the–CH_2OH group is considerably lower than its experimental value. In this work, the implicit-solvent effects were only considered by using the PCM model. The intermolecular interactions between two molecules of the **HL** Schiff base as well as between a **HL** molecule and molecules of the DMSO solvent have been omitted. However, the experimental chemical shifts were recorded in DMSO solution, in which the alcoholic H5 proton can engage in intermolecular hydrogen bonds with other **HL**

molecules and with solvent molecules of. The intermolecular interactions affect the chemical shift of the H5 atom.

The signal at 13.48 ppm is attributed to the H12 phenolic proton, which can be attributed to engagement of the H12 proton in intramolecular H-bond interaction with the N2 atom of the azomethine group.[15,20–22,24,41] A signal at 9.07 ppm is related to the H1 proton of the azomethine group. The aromatic protons cause several peaks at 6.69–8.01 ppm. However, the aliphatic protons of the $–CH_2OH$ and $–CH_3$ groups result in peaks at 5.54 and 2.46 ppm, respectively. The two protons of the $–NH_2$ amine group give rise to a triplet at about 4.79 ppm.

Vibrational spectroscopy

By comparing the DFT-computed and experimental vibrational frequencies, the IR spectra of the **HL** Schiff base and [Cu(**L**)Cl] complex were identified. Important results are gathered in Table S-III of the Supplementary material. In the 3600–2000 cm^{-1} region of the IR spectra of the investigated compounds, overlapping of the O–H, N–H and C–H stretching vibrations results in a broad band.[1,6,8,15,20–22,24] The deconvolution of this region of the IR spectra is listed in Table S-III. For the **HL** Schiff base, the stretching vibration of the phenolic O1–H12 bond appears at lower energies than the corresponding vibration of the alcoholic O2–H5 bond. This is related to the engagement of the H12 phenolic hydrogen in a intramolecular-hydrogen bond with the N2 atom.

The fingerprint region of the IR spectra of Schiff bases and their complexes is the 1660–1500 cm^{-1} region. The ν(C4=N2) causes a very intensive band at 1617 cm^{-1} of the IR spectrum of the **HL** Schiff base. By coordination of the N2 azomethine nitrogen to Cu^{2+}, this strong band shifts to lower energies by 12 cm^{-1}. However, deprotonation increases the electron density of the C1–O1 bond in [Cu(**L**)Cl] compared to the free **HL** Schiff base and the C1–O1 stretching vibration of the **HL** and [Cu(**L**)Cl] species appears at 1370 and 1421 cm^{-1}, respectively.[1,3,4,6,8,15,20–24] The appearance of two new bands at 547 and 640 cm^{-1} in the spectrum of the complex are attributed to the Cu–O and Cu–N bonds., which also confirm complex formation.

NBO analysis

The 3D maps of the highest-occupied-molecular orbital (HOMO) and the lowest-unoccupied-molecular orbital (LUMO) of the **HL** Schiff base and [Cu(**L**)Cl] complex are shown in Fig. 5. The HOMO orbital of the **HL** Schiff base is mainly localized on the benzene ring and its substituents. While its LUMO orbital is mainly localized on the pyridine ring and the azomethine group. The HOMO orbital of the [Cu(**L**)Cl] complex is mainly located on the pyridine ring, azomethine group and chloro ligand, while, its LUMO orbital is located on the two aromatic rings and the azomethine group.

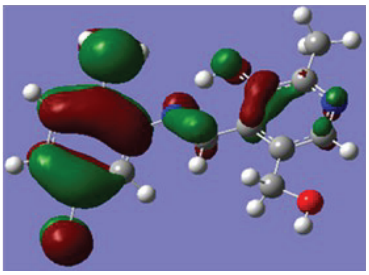
HOMO of **HL**

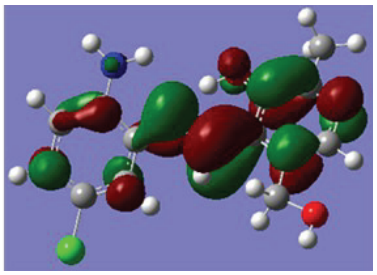
LUMO of **HL**

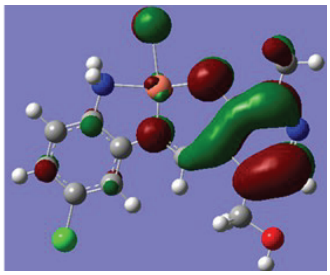
HOMO of [Cu(**L**)Cl]

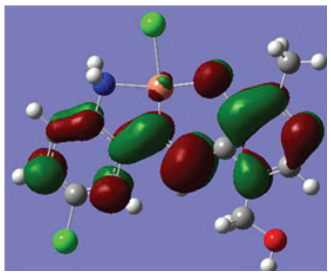
LUMO of [Cu(**L**)Cl]

Fig. 5. The HOMO and LUMO frontier orbitals of the **HL** Schiff base and its [Cu(**L**)Cl] complex.

The energy difference between the HOMO and LUMO frontier orbitals, energy gap, is one of the important characteristics of chemical compounds, which affects meaningfully on such cases as photochemical reactions, electronic spectra, *etc*. The calculated energy gaps for the **HL** Schiff base and [Cu(**L**)Cl] complex are 5.51 and 5.04 eV, respectively. These large energy gaps endorse the high stability of the investigated compounds.[1,6,15,20,21,24,41]

The NBO bond order of the C4=N2 bond is 1.91624 for the **HL** Schiff base, which decreases to 1.38736 in [Cu(**L**)Cl]. However, the NBO bond order of C1–O1 increases from 0.90019 in **HL** to 0.98852 in the complex. These calculated bond orders are in good agreement with the computed bond lengths and particularly the observed wavenumbers for stretching vibrations of these bonds in the IR spectra (Table S-III).

AIM analysis

The AIM molecular graphs of the **HL** Schiff base and the [Cu(**L**)Cl] complex are shown in Fig. S-4 of the Supplementary material, in which the small green spheres correspond to the BCPs. The calculated values for $\rho(r)$, $\nabla^2\rho$, H_b, G_b, V_b and $-G_b/V_b$ at the BCPs are listed in Table S-IV of the Supplementary material. In the **HL** Schiff base, the $\nabla^2\rho > 0$, $H_b < 0$ and $0.5 < -G_b/V_b < 1$ values demonstrate that the N2···H12 interaction is a medium and partially covalent intramolecular H-bond. As expected, the higher $\rho(r)$ demonstrates that the C4–N2

bond is stronger than the C9–N2 bond. In addition, the phenolic C1–O1 bond is stronger than the aliphatic C7–O2 bond.

Coordination of the N2 azomethine nitrogen decreases the calculated $\rho(r)$ values for the C4=N2 and C9–N2 bonds in comparison with the corresponding values in the free Schiff base. Furthermore, the $\rho(r)$ of the C10–N3 bond is decreased on coordination of the $–NH_2$ amine group to the Cu(II) metal ion. However, deprotonation of the O1 phenolic oxygen increases the $\rho(r)$ and strength of the C1–O1 bond in the complex. The calculated $–G_b/V_b$ values of the four coordinative bonds are about 1, confirming their covalent character. Based on the calculated $–G_b/V_b$ and H_b values, the Cu–N2 and Cu–Cl2 bonds are stronger and more covalent than the Cu–N3 and Cu–O1 bonds (Table S-IV).[34]

As seen in Fig. S-4, there are four rings in structure of the **HL** Schiff base: the benzene, the pyridine, a six-membered ring formed by the N2···H12 H-bond and a five-membered ring formed by the O2···H2 H-bond. The ring critical points (RCPs) of these rings are shown by small-red spheres. The computed $\rho(r)$ values for these rings are +0.021370, +0.023297, 0.018215 and +0.014036 $e^–/a_0^3$, respectively. Thus, the pyridine ring involves the highest electron density. In the optimized structure of [Cu(**L**)Cl], there are five different rings (Fig. S-4): the benzene, the pyridine, a five-membered chelate ring formed by the Cu–N2 and Cu–N3 bonds, a six-membered chelate ring formed by the Cu–N2 and Cu–O1 bonds and a six-membered ring resulting from the O2–H2 H–bond. The computed $\rho(r)$ values for these rings are +0.020589, +0.021327, +0.023384, +0.014097 and +0.015923 $e^–/a_0^3$, respectively. Thus, the highest electron density is attributed to the five-membered chelate ring formed by the Cu–N2 and Cu–N3 bonds.

Moreover, the $\nabla^2\rho > 0$, $H_b > 0$ and $–G_b/V_b > 1$ values confirm that the O2···H2 intramolecular H-bond is a weak, non-covalent interaction in the structures of both the **HL** and [Cu(**L**)Cl] species.[34] The energies of the N2···H12 and O2···H2 hydrogen bonds are –61.50 and –15.99 kJ $mol^{–1}$, respectively. Thus, the N2···H12 H-bond is much stronger than the O2···H2 one.

CONCLUSIONS

Based on the experimental analysis, only one amine group of the 4-chloro-*o*-phenylinediamine reacts with the pyridoxal to form the **HL** Schiff base, which may exist as two isomers: *para* and *meta*. On the other hand, each of the *para* and *meta* isomers has two different tautomers, the enol and the keto. The optimized geometries of the four possible tautomers of the **HL** Schiff base together with the kinetics and mechanism of its tautomerization were investigated theoretically. The experimental and the DFT-computed NMR results as well as the calculated energies approve that a methanol solution of the **HL** Schiff base contains only the enol tautomer of the *meta* isomer, which is the most stable tau-

tomer of **HL**. Good consistency between the DFT-calculated NMR chemical shifts and IR wavenumbers demonstrate the suitability of the optimized geometries for the **HL** Schiff base and the [Cu(**L**)Cl] complex. The NBO bond orders are also consistent with the vibrational frequencies of the IR spectra.

HL loses its phenolic proton to generate $\mathbf{L}^-$. Then, the $\mathbf{L}^-$ moiety acting as a tridentate ligand is coordinated to Cu^{2+} *via* the deprotonated-phenolic oxygen, the azomethine nitrogen and the amine nitrogen. The fourth coordination position of the square planar complex is occupied by a chloro ligand. The [Cu(**L**)Cl] complex has a more planar structure than the free **HL** Schiff base. The high-energy gaps between the HOMO and LUMO orbitals confirm the stability of both the investigated species.

The AIM analysis shows that the N2···H12 hydrogen bond of the **HL** Schiff base is a medium and partially covalent interaction, while the O2···H2 bond of the **HL** Schiff base and [Cu(**L**)Cl] complex is a weak and non-covalent hydrogen bond. In structure of the complex, the Cu–Cl2 and Cu–N2 bonds are stronger than the Cu–O1 and Cu–N3 bonds. Coordination of the N2 azomethine nitrogen and N3 amine nitrogen decrease the strength of the C4–N2, C9–N2 and C10–N3 bonds. However, deprotonation increases the strength of the C1–O1 bond. The pyridine ring and Cu–N2–C9–C10–N3 chelate ring have the highest $\rho(r)$ values in structure of the free **HL** Schiff base and [Cu(**L**)Cl] complex, respectively.

SUPPLEMENTARY MATERIAL

The optimized geometry of TSEnol–Keto, the optimized geometry and the Fukui map of the $\mathbf{L}^-$ species, the ^{1}H- and ^{13}C-NMR spectra of the **HL** Schiff base, the QTAIM molecular graphs of the **HL** and [Cu(**L**)Cl] species, the elemental analysis results, relative energies, assignment of the IR-vibrational frequencies and topological parameters of the investigated species are available electronically at the pages of journal website: http://www.shd.org.rs/JSCS/, or from the corresponding author on request.

ИЗВОД

(*E*)-4-(((2-АМИНО-5-ХЛОРОФЕНИЛ)ИМИНО)МЕТИЛ)-5-(ХИДРОКСИМЕТИЛ)-2-МЕТИЛПИРИДИН-3-ОЛ И ЊЕГОВ Cu(II) КОМПЛЕКС: СИНТЕЗА, DFT ИЗРАЧУНАВАЊА И AIM АНАЛИЗА

MORTEZA YAVARI, S. ALI BEYRAMABADI, ALI MORSALI и MOHAMMAD REZA BOZORGMEHR

Catalysis Technologies Development Division, Research Institute of Petroleum Industry, P. O. Box 14665-137, Tehran, Iran

У раду су новосинтетизовани Шифова база, (*E*)-4-(((2-амино-5-хлорофенил)имино)-метил)-5-(хидроксиметил)-2-метилпиридин-3-ол [**HL**] и њен [Cu(**L**)Cl] комплекс карактеризовани различитим спектроскопским методама. Поред тога, методи теорије функционала густине (DFT) су коришћени за истраживање таутомеризације **HL** Шифове базе, структурних параметара **HL** и [Cu(**L**)Cl] молекулских врста, решавање IR вибрационих трака и NMR хемијских помака, као и за анализе природних орбитала веза (NBO). Најстабилнији таутомер **HL** Шифове базе је енол облик *meta* изомера. Оптимизована геометрија слободне **HL** Шифове базе није планарна. $\mathbf{L}^-$ дејствује као N_2O тридентантни лиганд, који је везан за Cu^{2+} преко депротованог фенолног кисеоника, аминског и азо-

метинских азота. [Cu(**L**)Cl] комплекс има квадратну планарну геометрију, у коме хлоро лиганд заузима четврти координацијски положај. DFT израчунате вредности су у доброј сагласности са одговарајућим експерименталним вредностима, потврђујући прикладност оптимизованих геометрија **HL** и [Cu(**L**)Cl] молекулских врста. Сагласно високом енергетском јазу, ова једињења су стабилна. Анализа атома у молекулу (AIM) коришћена је за процену јачине везивних интеракција и електронских густина у структурама једињења.

(Примљено 10 октобра 2019, ревидирано 6 априла, прихваћено 26. априла 2020)

REFERENCES

1. A. A. A. Aziz, F. M. Elantabli, H. Moustafa, S. M. El-Medani, *J. Mol. Struct.* **1141** (2017) 563 (https://doi.org/10.1016/j.molstruc.2017.03.081)
2. P. Ghorbani, S. A. Beyramabadi, M. Homayouni-Tabrizi, P. Yaghmaei, *J. Serb. Chem. Soc.* **84** (2019) 1 (http://doi.org/10.2298/jsc190129055g)
3. C. Kanagavalli, M. Sankarganesh, J. Dhaveethu Raja, M. Kalanithi, *J. Serb. Chem. Soc.* (2018) 1 (https://doi.org/10.2298/jsc180521101k)
4. S. Saha, A. Das, K. Acharjee, B. Sinha, *J. Serb. Chem. Soc.* **81** (2016) 9 (http://doi.org/10.2298/jsc160425065s)
5. S. Sadeghi, A. Gafarzadeh, H. Naeimi, *J. Anal. Chem.* **61** (2006) 677 (https://doi.org/10.1134/s1061934806070136)
6. F. Jafari-Moghaddam, S. A. Beyramabadi, M. Khashi, A. Morsali, *J. Mol. Struct.* **1153** (2018) 149 (https://doi.org/10.1016/j.molstruc.2017.10.007)
7. K. C. Gupta, A.K. Sutar, *J. Mol. Catal., A* **272** (2007) 64 (https://doi.org/10.1016/j.molcata.2007.03.025)
8. E. G. Bakirdere, M. F. Fellah, E. Canpolat, M. Kaya, S. Gür, *J. Serb. Chem. Soc.* **81** (2016) 12 (http://doi.org/10.2298/jsc151030008b)
9. M. Gaber, H. A. El-Ghamry, S. K. Fathalla, M. A. Mansour, *Mater. Sci. Eng., C* **83** (2018) 78 (https://doi.org/10.1016/j.msec.2017.11.004)
10. N. Ribeiro, S. Roy, N. Butenko, I. Cavaco, T. Pinheiro, I. Alho, F. Marques, F. Avecilla, J. Costa Pessoa, I. Correia, *J. Inorg. Biochem.* **174** (2017) 63 (https://doi.org/10.1016/j.jinorgbio.2017.05.011)
11. P. Sukanya, C. Venkata Ramana Reddy, *Appl. Organomet. Chem.* **32** (2018) e4526 (https://doi.org/10.1002/aoc.4526)
12. K. Dhahagani, M. P. Kesavan, K. Gujuluva Gangatharan Vinoth, L. Ravi, G. Rajagopal, J. Rajesh, *Mater. Sci. Eng., C* **90** (2018) 119 (https://doi.org/10.1016/j.msec.2018.04.032)
13. G. Anbarasu, M. Malathy, P. Karthikeyan, R. Rajavel, *J. Solid State Chem.* **253** (2017) 305 (https://doi.org/10.1016/j.jssc.2017.06.012)
14. M. Aghajani, N. Monadi, *Appl. Organomet. Chem.* **32** (2018) e4433 (https://doi.org/10.1002/aoc.4433)
15. H. Eshtiagh-Hosseini, M. R. Housaindokht, S. A. Beyramabadi, S. H. M. Tabatabaei, A. A. Esmaeili, M. J. Khoshkholgh, *Spectrochim. Acta, A* **78** (2011) 1046 (https://doi.org/10.1016/j.saa.2010.12.045)
16. J. Berg, L. Stryer, *Biochemistry*, WH Freeman and Company, New York, 2002
17. J. S. Hartman, E. C. Kelusky *Can. J. Chem.* **57** (1979) 2118 (https://doi.org/10.1139/v79-340)
18. G. C. Lakshmi, S. Ananda, N. M. M. Gowda, *Synth. React. Inorg. Met.-Org. Nano-Metal Chem.* **39** (2009) 434 (https://doi.org/10.1080/15533170903227796)

19. H. Brurok, J. H. Ardenkjær-Larsen, G. Hansson, S. Skarra, K. Berg, J. O. G. Karlsson, I. Laursen, P. Jynge, *Biochem. Biophys. Res. Commun.* **254** (1999) 768 (https://doi.org/10.1006/bbrc.1998.0131)
20. S. Beyramabadi, A. Morsali, A. Shams, *J. Struct. Chem.* **56** (2015) 243 (https://doi.org/10.1134/S0022476615020067)
21. S. A. Beyramabadi, A. Morsali, M. J. Khoshkholgh, A. A. Esmaeili, *Spectrochim. Acta, A* **83** (2011) 467 (https://doi.org/10.1016/j.saa.2011.08.067)
22. S. A. Beyramabadi, M. Khashi, A. Morsali, A. Gharib, H. Chegini, *J. Struct. Chem.* **59** (2018) 1326 (https://doi.org/10.1134/S0022476618060112)
23. M. Yavari, S. A. Beyramabadi, A. Morsali, M. R. Bozorgmehr, *J. Struct. Chem.* **59** (2018) 1102 (https://doi.org/10.1134/s0022476618050128)
24. S. Beyramabadi, A. Morsali, S. Vahidi, M. Khoshkholgh, A. A. Esmaeili, *J. Struct. Chem.* **53** (2012) 460 (https://doi.org/10.1134/S0022476612030079)
25. M. Frisch, G. Trucks, H. Schlegel, G. Scuseria, M. Robb, J. Cheeseman, J. Montgomery Jr., T. Vreven, K. Kudin, J. Burant, *Gaussian 03, revision B. 05;* Pittsburgh, PA, 2003
26. C. Lee, W. Yang, R. G. Parr, *Phys. Rev., B* **37** (1988) 785 (http://doi.org/10.1103/PhysRevB.37.785)
27. P. J. Hay, W. R. Wadt, *J. Chem. Phys.* **82** (1985) 270 (https://doi.org/10.1063/1.448799)
28. R. Cammi, J. Tomasi, *J. Comput. Chem.* **16** (1995) 1449 (https://doi.org/10.1002/jcc.540161202)
29. R. Ditchfield, *Mol. Phys.* **27** (1974) 789 (https://doi.org/10.1080/00268977400100711)
30. D. C. Young, *Computational Chemistry: A Practical Guide for Applying Techniques to Real World Problems*, Wiley Online Library, New York, 2001
31. T. A. Keith, *TK Gristmill Software,* Overland Park, KS, 2013
32. R. F. W. Bader, *Chem. Rev.* **91** (1991) 893 (https://doi.org/10.1021/cr00005a013)
33. E. Espinosa, M. Souhassou, H. Lachekar, C. Lecomte, *Acta Crystallogr., B* **55** (1999) 563 (https://doi.org/10.1107/S0108768199002128)
34. I. Rozas, I. Alkorta, J. Elguero, *J. Am. Chem. Soc.* **122** (2000) 11154 (https://doi.org/10.1021/ja0017864)
35. A. Soroceanu, M. Cazacu, S. Shova, C. Turta, J. Kožíšek, M. Gall, M. Breza, P. Rapta, T. C. O. Mac Leod, A. J. L. Pombeiro, J. Telser, A. A. Dobrov, V. B. Arion, *Eur. J. Inorg. Chem.* **2013** (2013) 1458 (https://doi.org/10.1002/ejic.201201080)
36. M. Sankarganesh, N. Revathi, J. D. Raja, K. Sakthikumar, G. G. Vinoth Kumar, J. Rajesh, M. Rajalakshmi, L. Mitu, *J. Serb. Chem. Soc.* **83** (2018) 1 (http://doi.org/10.2298/jsc180609080s)
37. S. Noor, S. Kumar, S. Sabir, R. W. Seidel, R. Goddard, *Acta Cryst., E* **71** (2015) m205 (https://doi.org/10.1107/S205698901501960X)
38. H. Kargar, R. Kia, T. Shakarami, M. N. Tahir, *Acta Cryst., E* **68** (2012) m752 (https://doi.org/10.1107/S1600536812020387)
39. L. Yang, D. R. Powell, R. P. Houser, *Dalton Trans.* **2007** (2007) 955 (https://doi.org/10.1039/B617136B)
40. A. Kanaani, D. Ajloo, G. Grivani, A. Ghavami, M. Vakili, *J. Mol. Struct.* **1112** (2016) 87 (https://doi.org/10.1016/j.molstruc.2016.02.024).